Pressure Measurement on the Sidewall of a Supersonic Nozzle Using Pressure Sensitive Paints

Christopher Garrett[1]

University of New South Wales at the Australian Defence Force Academy

Whilst pressure sensitive paints have become a mature method of pressure analysis their application with UNSW Canberra has been limited in exposure. This report aims to describe the analysis conducted in order to verify PSPs as an accurate, fast and costly method of data reduction to identify the pressure distribution for a specimen subjected to a flow field. Our chosen specimen was an over-expanded supersonic nozzle. The intensity ratio system of image processing showed agreeable results with the expected flow field resolved from CFD and schlieren image solution. A study on the 2D transverse assumption of the nozzle showed good agreement from the transverse pressure distribution. A comparative study of two forms of the chosen Stern-Volmer equation showed the linear solution to provide a more accurate solution to our Fourier series solution. The temperature dependency of the PSP was analysed and the degree of dependency shown to have an effect on time-step images taken from the same run-case. Whilst the intensity ratio system provided results with a good agreement, the analysis was conducted within a range of specific conditions which matched the chosen method. The requirement for a method of temperature correction, in the case the use of pressure taps, limits the application of this system. A decay-based system should be explored and the potential development of a binary paint investigated.

Contents

[1] LT, School of Engineering & Information Technology. ZEIT4501.

Nomenclature

Terms:

PSP	=	pressure sensitive paint
TSP	=	temperature sensitive paint

Variables:

I_{ref}	=	luminescence intensity at reference condition
I	=	luminescence intensity at desired condition
$A(T), B(T), C(T)$	=	Stern-Volmer coefficients
P_{ref}	=	static pressure at reference condition (kPa)
P	=	calculated pressure at desired condition (kPa)
T	=	temperature (K)

I. Introduction

A. Motivation

The motivation for this project comes from the introduction of PSPs within UNSW Canberra. Whilst the development and application of PSPs have been accepted as a mature method of pressure analysis, there has been limited exposure within the university itself. This project was set to analyse a viable method of application and processing within the constraints identified. This would provide a method for the use of PSPs from the initial study performed and allow a wider application throughout UNSW Canberra with the potential for alternative data-reduction methods.

Traditionally, arrays of thermocouples and pressure transducers were used to obtain surface temperature and pressure distributions. However, these techniques are often labour intensive and require high preparation costs to prepare the specimen. This is coupled with the limitations introduced due to the number of instrument locations required for spatial resolution and their respective difficulties in the manufacturing process. Comparatively, PSPs are a simple, inexpensive means of full-field measurement with the potential for high spatial resolution[i]. PSPs also provide the advantage of continuous field measurement over complex surfaces such as sharp corners, backward steps and curved surfaces where pressure taps become impractical or costly[ii].

Specifically, this project will look at measuring the effectiveness of the paint as a pressure measurement system when applied to an over-expanded, supersonic nozzle designed by PhD student Kyll Schomberg. Through literature review a data reduction method was identified which would be suitable for the test conditions. A comparative study was made using calculated solutions in order to identify the viability of the resolved solution. A study was conducted on the accuracy of two forms of the Stern-Volmer equation to determine which provided more reasonable results and the 2D transverse assumption was analysed. A time-analysis study was also conducted in order to determine the temperature dependency of the paint, which was identified as the leading cause of discrepancy in the calculated solution.

B. Aim

The aim of this project was to identify a method of data reduction and conduct a study of the pressure measurements calculated to determine the viability of the paint as a pressure measurement system. The project would also document the chosen method of analysing the PSPs. At the conclusion of this project verified results were obtained and the primary sources of error identified. The Intensity Ratio method was shown as a viable method of data reduction and showed good agreement with expected results. This project was also used to ascertain other data reduction methods of interest for further studies, in particular the Decay based method and use of a binary paint system.

II. Literacy Review

A. Background

Pressure Sensitive Paints (PSPs) refer to a sensor system where paint is illuminated and its luminescence measured in order to determine information on pressure due to the environment the paint is subject to[iii]. They can provide a non-intrusive measurement system over a wide spatial area at a high spatial resolution. This large spatial resolution reduces the requirement to interpolate data between pressure taps. The results captured can provide both qualitative and quantitative information of the pressure distribution across the surface of the specimen. As will be discussed later it will be seen that pressure trends can be determined quickly with little

processing. However, for a more accurate pressure distribution the images taken must be subjected to post-processing. Fig. 1 shows the typical set-up for a PSP measurement system.

Measurements are done through luminescing molecules within the paint which can be excited to higher levels of energy. This excitation energy is typically in the range of 300-500 nm (green to ultraviolet range) and is released as the electron returns to its lower energy level through the emission of photons. This emission is in a different range to that of the excitation source. This is to reduce the introduction of noise error due to capturing energy from the emission source. For the paint used, the emission range was 470 nm. This emission can however, be quenched by exposure to oxygen. Its presence provides an alternative method of energy loss due to the small molecule size, high diffusivity and energy-level structure of O_2. As the emission process is dependent on the paints exposure to oxygen, we can calibrate the paint in terms of the local oxygen concentration, and therefore the local pressure[iv].

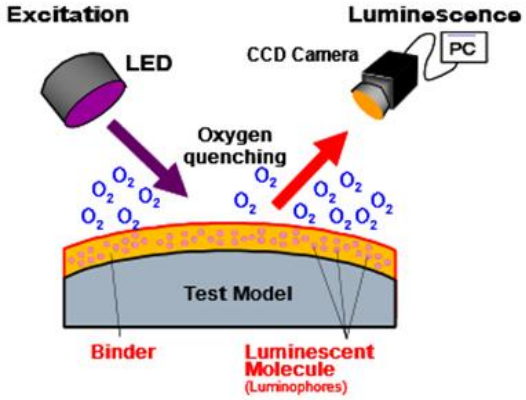

Figure 1. Diagram representing PSP measurement system.

This dependence on the absorption of photons by the local oxygen concentration also makes the process dependent on the local temperature. As temperature rises, the energy level of the oxygen molecules are raised which affects the rate of absorption. The degree of error introduced due to temperature is the largest source of error within the system and often requires calibration during the experimental stage[v]. Furthermore, internal chemical reactions are more likely to occur at higher temperatures. This provides a limit to the range in which the PSP can be applied as it causes internal energy conversion and a relaxation process where energy is lost not through either the luminescing or quenching process. This is largely dependent on the chemical composition of the paint itself and will either be provided by the manufacturer or can be determined experimentally.

The relationship described gives an inverse correlation where the higher the local pressure, the greater the local oxygen concentration within the same spatial system but the lower the emission that is measured due to the quenching effect. The luminescing molecules are contained within a porous binder material. This allows the local oxygen concentration to permeate into the paint to enact the quenching process. Both the paint layer and the polymer binder material can both be dissolved in a solvent. This resulting paint is then applied to the test surface through a brush or sprayer.

B. PSP Measurement Systems

There are two primary systems associated with the measurement of PSPs. These are intensity and decay systems. As outlined, the chosen method was the intensity system. Both have common limitations; only visible areas can be measured, and the excitation source and camera must remain outside of the flow field. In wind tunnel measurements a window is required. This can limit the areas of interest which may be desired. For example, areas on a wing near the nacelle will be difficult to view from outside the tunnel. The camera may be placed within the tunnel itself; however, this cannot interrupt the flow field for the desired test region.

The intensity based method is a mature method with a number of studies. It has a number of advantages over the decay based method but comes with a number of requirements that limit its application. The intensity based method requires a form of temperature correction[vi]. This is often done through pressure taps when available. Values at the pressure taps can be used to determine the Stern-Volmer constants, and therefore the temperature correction factor across the test surface. This correction factor is then interpolated across the entire surface. This ideally requires the taps to be placed close to the boundaries of the test surface to reduce the requirement for data extrapolation which would introduce further uncertainty to the results at these regions.

Another method of temperature correction is through the use of an IR camera. This would require the surface of the model to be mapped out and corresponding pixel positions adjusted. This would require an *a prior* calibration in order to determine the temperature constants for a known temperature and pressure. This is generally considered the least accurate of the methods as it would require greater interpolation between data sets. Furthermore, the dependency of the paint on temperature is not linear and can change as the paint approaches the temperature limits. The third method is to use a binary paint system. This is where the paint contains both pressure independent and dependent luminophores. As with the IR camera method this will give us a correction factor to apply across the test surface but can be done for each test case and does not require a calibration. For the experiment pressure taps were already made in the forming process and therefore available.

The primary advantage of the intensity based method is the ability to account for a number of discrepancies due to non-homogenous surface results due to illumination, camera noise, and paint thickness. Any moisture or condensation on the surface of the paint can form a barrier. However the intensity method requires the division

of the intensity image at the reference state by the run state. Therefore by measuring these at ideally the same conditions any non-ideal effects are removed as only the difference between each relative pixel position is described[vii]. Other effects will be examined throughout the report as they pertain to each stage of the experiment. In order to analyse the captured intensity images we need a relationship between the captured emission and the pressure on the surface of the model. Eq. (1) shows the Stern-Volmer equation where a direct relationship is formed from the intensity ratio I_{ref}/I and P/P_{ref}.

$$\frac{I_{ref}}{I} = A(T) + B(T)\,\frac{P}{P_{ref}} \qquad (1)$$

This form requires an amount of complexity within the Stern-Volmer coefficients in order to account for the non-linear effects between pressure and temperature dependencies. Another method analysed was through a Fourier series transformation to attribute non-linear characteristics within the pressure terms, as shown at Eq. (2).

$$\frac{I_{ref}}{I} = A(T) + B(T)\,\frac{P}{P_{ref}} + C(T)\left(\frac{P}{P_{ref}}\right)^2 + \cdots \qquad (2)$$

For the purposes of the test case, both Eq. (1) and (2) were examined and results comparatively analysed.

The decay system allows the measurement of pressure to become independent of a reference condition. It uses a pulsed light source to excite the luminophores. The rate of decay of the emission is then measured. However, studies have shown that accuracy and speed of measurement are reduced in comparison to the intensity based method and that results were not repetitive due to dispersion in the rates of decay due to inhomogeneous environments[viii]. It was also determined unsuitable for the experiment due to the over expanded flow field. The flow field develops over time, making it difficult to ascertain that the decay rate measured was a function of the initial pressure and independent of the changes in pressures over the surface.

III. Calibration

A. Experimental Set-up

The area of interest on the test model is illuminated with an excitation source. Ideally this should be at constant illumination intensity. However in the intensity ratio method this is largely mitigated as the intensity at each spatial coordinate is taken for all captured images. However the model should ideally remain within the same spatial coordinate system for both the reference and wind-off case[ix]. Another solution is to mount the camera on the model to account for any deflection. This is however, largely dependent on each individual experimental case. If neither of these conditions is true, the images will have to undergo image processing in order to align both cases. For the purpose of the supersonic nozzle rig the nozzle was held in a block and remained spatially constant throughout each run time. For the experiment an LED light was chosen as it ideally provides a near ideal distribution of lighting. In order to run a more sensitive analysis the excitation source may require a laser light system. However this will require calibration in order to illuminate the entire model. This can present further sources of error due to a non-uniform distribution of light.

In order to capture the emission from the PSP a camera with a mounted red-filter was set-up. This set-up could have been refined with a red-filter camera lens rather than the red sheet used. Whilst the red-filter reduced the captured energy emission to the red-spectrum a purpose designed lens for the 470 nm spectrum would have further reduced any noise due to the capturing process. This was not used as it was unavailable for the test. The error introduced here is due to Stokes Shift. This occurs when the energy of the excitation source is higher than that of the emission. The red-filter removes the captured excitation energy, leaving the captured image primarily due to emission[x]. Background illumination effects must also be largely eliminated. Illumination was reduced from local light sources and any devices with illumination set-up so that they would not directly impede on the emission path. The camera itself can introduce noise discrepancy effects. The ability of the camera to capture emitted photons and attribute this information to each pixel spot can have an effect on the noise generated during the capturing process. This is reduced with the quality of the image captured and the image resolution. As described above this effect becomes less pronounced as the excitation source signal is increased in intensity, increasing the emission signal in respect to background effects.

Due to the geometry of the nozzle rig itself, there was a restriction on where both the excitation source and camera could be placed. The experiment restricted observation to the nozzle to either side of the rig as shown in Fig. 2. This meant that both were at an angle of attack to the nozzle surface in question. Ideally both would be placed perpendicular to the surface in order to create and ideal distribution of excitation and captured emission. This would further ease the post-processing workload. However, the use of the intensity ratio method reduced any introduced error due to the non-ideal set-up case.

For the case study the nozzle was held within a stationary block. We were able to confidently ascertain that there would be minimal displacement during the run case. Any deflections were identified through pressure transducers mounted to the model to detect any potential movement of the rig. It was determined that any movement in the model would have had negligible effects due to the construction of the nozzle block itself. The nozzle rig is shown in Fig. 2.

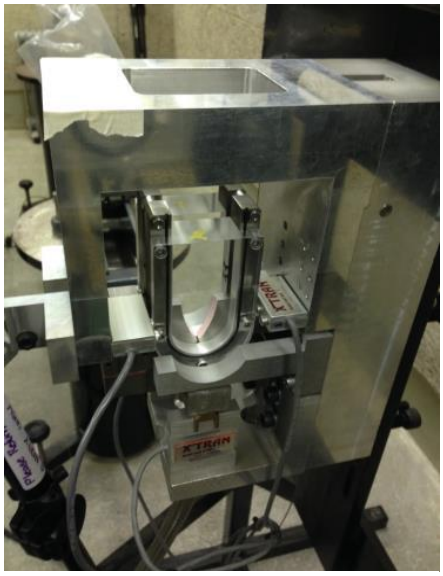

Figure 2. Supersonic Nozzle Rig.

The block was designed so that the central segment, as defined by the sidewall Perspex windows, could be removed. This was to allow easy changes of the nozzle design for consecutive experiment runs. The Perspex windows were introduced to eliminate the effect of the flow to a 2D case. This assumption was analysed and is shown later in the report. This was primarily done for ease of evaluation of Schlieren and CFD results by Kyll Stromberg. The Perspex windows did however introduce a new source of error. Due to the effects of prolonged use the windows were lightly abraded. Again this effect became negligible due to the ratio method chosen. Any error introduced by abrasion was reduced when the ratio of intensities was taken. This error could have been removed with the introduction of glass windows. However, this was discounted fairly early in the project due to high costs for the required materials. The glass would have to be constructed with respect to the high pressure cases they would be subject to as well as be functional for Schlieren measurements.

The nozzle itself was prepared in an acetone and ultrasonic bath. This was done to remove the introduction of debris and flash due to the manufacturing process, exposure within the workshop and from previous use. The paint was applied through a sprayer. This allowed the paint to be applied more uniformly[xi]. However, as was discovered during the run cases of the experiment the thinner paint layer produced wore away due to exposure within the flow field. This caused areas of chipped and abraded paint. These areas were primarily focused on the edges of the nozzle surface where it met with the Perspex sidewalls. As will be discussed in the post-processing these areas were largely ignored in the final results due to further introduced errors. Whilst brushing the paint should mitigate this effect due to a stronger developed bond between the pain and nozzle surface, it can create additional error effects. A non-homogeneous layer of paint can be intrusive on the flow field due to changes in the surface of the model and may affect the emission process. In extreme cases the flow field can become altered due to ridges and troughs introduced due to the paint. On larger surfaces this effect becomes less pronounced. Differences in intensities caused by changes in thickness of the paint are mitigated by the intensity ratio method.

B. Calibration Methods

A number of calibration methods were researched and analysed by Woodmansee, M. and Dutton, J. where results were compared to pressure tap measurements. *Isothermal* calibration assumes the surface is spatially and temporally isothermal. Whilst the simplest of the methods, it under predicted all pressure tap measurements as it did not account for the temperature drop from the reference condition. *A priori* calibration places a sample of PSP within a vacuum chamber. The chamber is then controlled to desired conditions in order to determine the temperature relationship. This method was deemed unsuitable as a dedicated pressure chamber was unavailable. *In situ* calibration relies on the available pressure taps for temperature correction. The intensity measured around the pressure taps is used to form a calibration curve. This was found to be the most accurate method as the measurements coincided closely with pressure tap readings. *K-fit* calibration uses both isothermal and *in situ* calibrations and is performed when pressure taps are limited and do not span a large enough area in order to use just the in-situ method. Whilst the isothermal assumptions are less severe than in *isothermal* calibration, there was a large deviation in results as distance from the pressure taps increases. Table 1. shows the calculated uncertainty as analysed by Woodmansee and Dutton[xii].

Table 1: Percentage differences between pressure tap measurements and data reduction methods (full scale\250 kPa)[xiii]

	Isothermal	In-situ	K-fit
Mean	8.00	1.03	4.68
RMS	2.84	0.55	2.72
Maximum	11.03	2.14	7.52
Minimum	1.38	0.26	0.36
Pressure Uncertainty	1.58	0.96	1.96

IV. Results

A. Case Study

A number of experimental results were obtained over a range of inlet or throat pressure ratios in conjunction with the PSP. For the purposes of this report a single case study will be examined and reviewed. The nozzle was designed for high inlet pressure ratios. However this would have taken the measurable range outside of the defined limits for the paint, as set by the manufacturer. Therefore the nozzle had to be run at relatively low inlet pressure ratios. This had the effect of causing the flow to develop into an over-expanded flow. Whilst this made the flow more difficult to measure quantitatively, as theoretical calculations of the flow condition became computationally complicated, the flow could be qualitatively examined. The flow produced a discernible patterned pressure region effect.

The inlet pressure ratio of the nozzle was nominally set to a pressure ratio of 5, 10, 15 and 20 bar. For the purposes of the analysis done in this report the KS10 nozzle was examined at PR 11.531 bar. This will be referred to as the 10 bar case. A single case would allow a more effective analysis of the assumptions and effects on the nozzle surface. Pressure was set at four G size air canisters through a pressure regulator. The pressure was recorded and each test case was run for at least 10 seconds in order to allow for changes in temperature to be recorded and for quasi-stead flow conditions to be met[xiv].

B. Pressure Calculation

In order to determine the pressure distribution across the sidewall face of the nozzle the captured images had to undergo post-processing. Fig. 3. shows the captured image through the red-filter lens. In all cases the test case, or wind-on image, was used with the reference, or wind-off, image. This reference image is captured at a known condition, in the case this is atmospheric conditions. The wind-off case image is dived by the wind-on case. The experiment would see an increase in the pressure distribution across the surface. From the relationship derived early we can see that this would result in an overall drop in the image intensity. In order to further eliminate any captured noise, the image was reduced to only the red spectrum. This was to reduce light captured from external illumination sources. Whilst this should be reduced in the image division it serves to reduce any changes in intensity due to external illumination changes.

Figure 3. Nozzle surface with applied PSP through red-filter.

The calculated result gives us the I_{ref}/I. From here pressure measurements recorded at the pressure tap locations were recorded. In order to determine the Stern-Volmer coefficients the intensity ratio at a point adjacent to the pressure tap was chosen. This was taken at a point where the pressure tap itself would not affect the intensity of the pixel but where there would be minimal changes in intensity from the nominal pressure tap position. Whilst this can introduce a degree of uncertainty in the calculations the intensity variation around the chosen point was within a variation of ±2%. This process was found to be a laborious task as the location around the pressure tap had to be examined in order to determine where the value would be taken.

From here the Stern-Volmer coefficients were determined at each pressure tap location and the average calculated for the nozzle sidewall. This is through satisfying the Stern-Volmer equations as simultaneous equations using the measured pressures and intensity ratios. A calibration curve would have provided more satisfying results. Whilst these values should ideally be the same, they are a function of the paint itself, in the test case there was a predicted temperature variation across the surface of the nozzle. This is due to the thermal induction across the nozzle surface the flow development through the nozzle. It was therefore predicted that as the flow developed laterally the temperature should decrease. However, it was noted that through the use of an IR camera during the run-time that there was a negligible change in spatial surface temperature during the run-time. The calculated coefficients were then input into the Stern-Volmer equation at each intensity location for the measured face. This was used to determine the static pressure, P, across the nozzle surface.

C. Image Processing

In order to smooth out the presence of outlier results due to noise effects on the calculated pressure distribution image a linear filter was applied. This took the surrounding eight pixels at each location on the image and resolved the new value as an average of the total nine calculations. Fig. 4. shows an example of this process where the pixel, defined $x_{m,n}$ is transformed to the value $y_{m,n}$.

An analysis was performed to determine whether this would cause a loss in the accuracy of the solution. The method used inherently causes an imperfect solution at the boundaries of the captured image. This is due to the presence of empty data surrounding the boundary pixels. However, as we move further from the image boundary this effect because less pronounced and has a negligible effect on the nozzle surface data. This effect was highlighted where NaN or Inf results were recorded due to intensity measured outside of the PSP region. The filter effect expanded these outlier regions. Table 2. shows corresponding sample results before and after the filter was applied in the first recorded high pressure region. Note pixel values were reduced to three decimal places to ensure readability.

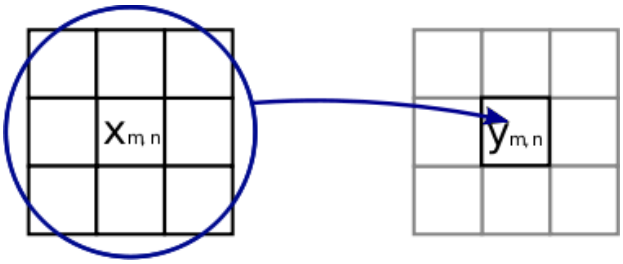

Figure 4. Example of the filter process applied.

Table 2: Comparison of pre- and post-filter effects of pressure distribution of 10 bar case.

Pressure (kPa), pre-filter results		
247.541	247.541	247.541
280.942	280.942	274.114
Pressure (kPa), post-filter results		
260.242	257.916	257.405
269.833	267.533	263.995

As shown there is recorded change in some of the measured results. In the example shown, the corresponding values shown in the second rows undergo a transformation of up to 5% from the original value. When examined in the wider context of the image, these results were outliers, as shown by the sudden increase in ~33.4 kPa from adjacent pixels. However, after undergoing the filter process, this drop becomes less significant with a raise of only ~9.5 kPa recorded. The first row also undergoes a transformation of 4.19%. However this is largely due to the presence of the outlier results and it was noted that this effect becomes less pronounced after only a few iterations above the examined area. After examining the two images, generated from both sets of results, there is little qualitative deviation seen.

The resolved intensity ratio image provides a qualitative look at the distribution of pressure across the surface of the nozzle, albeit with an inversed distribution where higher intensity pixels correlate to a lower pressure value. This can provide a quick tool to gain a small measure understanding of the characteristics of the flow. Fig. 5. shows the intensity ratio of the nozzle surface of the 10 bar case. Once we have attributed the image processing described above we can now view the image in a quantitative sense. Attributing the colourbar to correspond to the image gives us the values for the pressure distribution. Further information can be drawn from this by finding the data set values that correspond to each pixel spot shown. Fig. 6. shows the calculated pressure distribution for the 10 bar case.

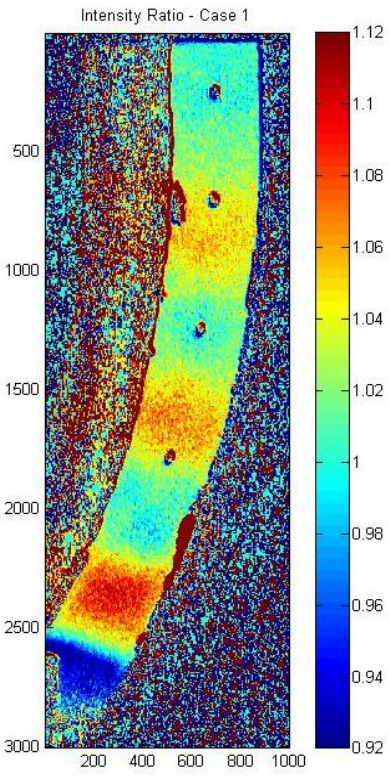

Figure 5. Intensity Ratio image of 10 bar case.

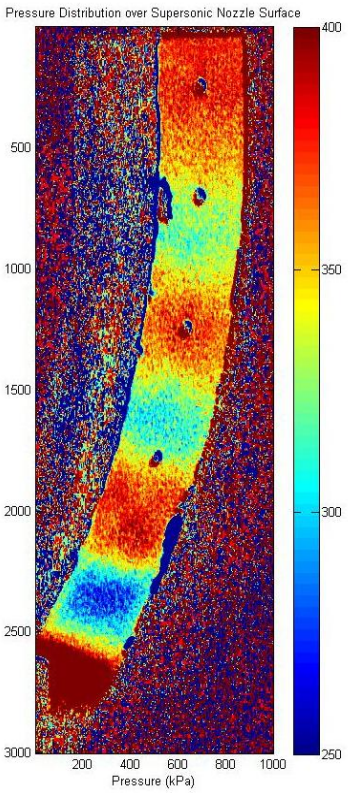

Figure 6. Pressure Ratio image of 10 bar case.

It is worth noting that for the images there is a large distribution of noise outside of the nozzle surface. This is simply due to outlying results where some source of signal was measured where no PSP was present. Whilst a simple cropping tool was used to reduce the image down to the area in question, a further development on this process would be to redistribute the matrix data so that the image is formed into a representational shape looking perpendicularly at the nozzle. It was decided that whilst this would be useful to alleviate the difficulty in analysing the image from the angular view it currently shows, it would not provide any additional information that would contribute to the analysis conducted. Furthermore, it would likely require either the elimination or converging of existing data or the interpolation of data in other areas in order to form the desired view. Methods that were investigated showed that this process is highly dependent on the image itself and that any program developed would need to be catered for each test case.

Whilst initial PSP results showed good agreement with both schlieren and CFD results, there were a number of measured discrepancies. Due to the set-up of the canisters there was a degree of uncertainty in the pressure at the inlet of the nozzle. This was due to pipe losses experience by the flow. There was also a degree of difficulty in manually calibrating each of the four canisters so that they would provide an equal contribution to the flow. This manual process made it difficult to accurately adjust the flow to the required condition. Difficulties in measuring the time at which the images were captured make the comparison with experimental results difficult to confirm. Images were taken manually and thus could not be accurately correlated with a time at each step. Fig. 7. shows the CFD and schlieren results and was used in order to qualitatively analyse the flow field[xv].

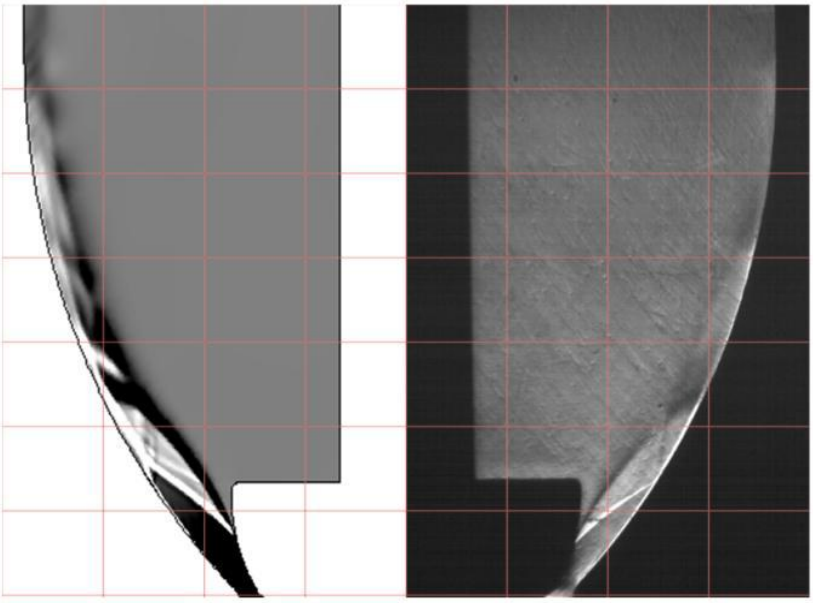

Figure 7. CFD and schlieren images of flow field of 10 bar case.

As shown there was a good agreement between the expected flow field and the results measured by the PSP. The shock pattern resulting from the over-expanded flow and artificial nozzle separation, a function of the nozzle shape, was shown in the formation of consecutive high and low pressure regions. There results indicate that a high frequency thrust and flow structure variation were present. Whilst the unsteady shock patterns expected were not measured directly from the PSP images, they were evident when images were examined over as a function of time.

D. **Transverse Assumption**

In order to ascertain the validity of the results an analysis of the 2D assumption was performed. This was done by measuring the transverse pressure deviation across the nozzle surface. A sub-function was developed that would allow the user to select the values to measure and plotted these against one another. This was done in order to measure the deviation of results obtained transversely across the nozzle. Fig. 8. shows a scatter graph of the transverse measured pressures.

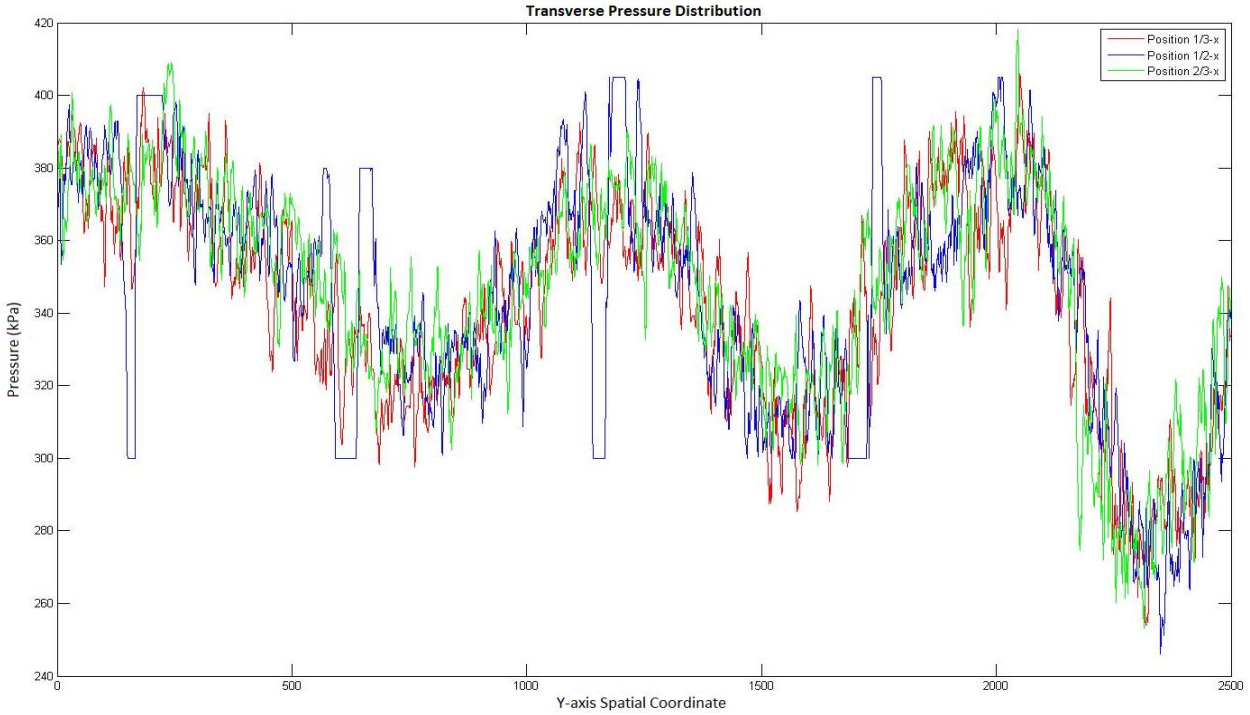

Figure 8. Comparison of the transverse pressure distribution of 10 bar case.

Measurements were taken nominally at 1/3, 1/2, and 2/3 positions, measured laterally from the left-hand side of the nozzle surface. It is worth noting that there were a number of outlier results that were reduced due to measurements from the ½ transverse width that captured intensity from within the pressure taps. Table 3. shows a distribution of these values and the measured transverse deviation of results at corresponding points along the nozzle.

Table 3: Comparison of the transverse pressure distribution and deviation of 10 bar case.

Y-axis Spatial Coordinate	Pressure (kPa) – 1/3 Transverse Position	Pressure (kPa) – 1/2 Transverse Position	Pressure (kPa) – 2/3 Transverse Position	Max. Deviation – kPa/%
500	365.434	353.456	371.757	6.323/1.73
1000	337.527	324.684	348.112	23.428/7.22
1500	326.413	314.213	324.719	12.20/3.88
2000	371.348	396.969	395.441	25.621/6.90

Upon examination of the transverse edges of the nozzle surface we can see there is a noticeable change in pressure. The effect is more pronounced in the relatively low pressure regions and is generally transitional. The effect of having the Perspex sidewalls causes the formation of an additional set of boundary layers. Whilst this nominally does not change the pressure distribution through the flow path it can have an effect on the temperature distribution. However, the formation of a thermal boundary layer had negligible effects. Images taken from IR camera measurements showed a tendency towards a state of thermal equilibrium across the nozzle surface. As examined above, the 2D transverse assumption shows us that the flow is relatively consistent transversely. Therefore, we can ascertain that this effect derives from a function of the diffusive effect of the flow field from the Perspex windows. For the purpose of the transverse study these regions, whilst only ~5% transverse thickness either side of the nozzle surface was effected, the regions were not examined due to these effects.

The results show a maximum deviation of 7.22%. This highlighted that the pressure obtained from the positions either side of the central line of the transverse length were more agreeable to the pressure trend. This is likely an error caused by noise emission captured from the pressure tap holes. This error is further accentuated by the smooth filter applied. However all results show a fairly consistent result with the deviation ranging from 1.73-7.22%. This shows that the transverse assumption is fairly accurate in the given conditions. However the deviation measured is likely due to the aforementioned losses experience by the flow by the Perspex windows and their interference with the shock interactions.

E. Method Comparison

The results shown were all derived from computationally solving the linear model at Eq. (1). In order to determine whether this method gave a more accurate solution a comparison of the two methods shown was made. Fig. 9. shows the solution when attributed to Eq. (2).

As can be seen the results from the Fourier series model equation tended towards a more extreme spread in the pressure distribution. This was likely due to the distribution of pressure from the lack of a calibration curve of results. This caused calculations to fluctuate more greatly as the temperature correction coefficients were unsuitable. In the Fourier series model the non-linear properties of the flow are attributed within the pressure distribution ratios. However, the linear solution fits these non-linear tendencies into the two constants, *A(T)* and *B(T)* and surprisingly gives much more agreeable results. This was reinforced by deviation studies performed. The Fourier series model showed a tendency to deviate by ~13% in its transverse pressure distribution. The filtering process was also much more extreme with pressure drops of ~13% calculated.

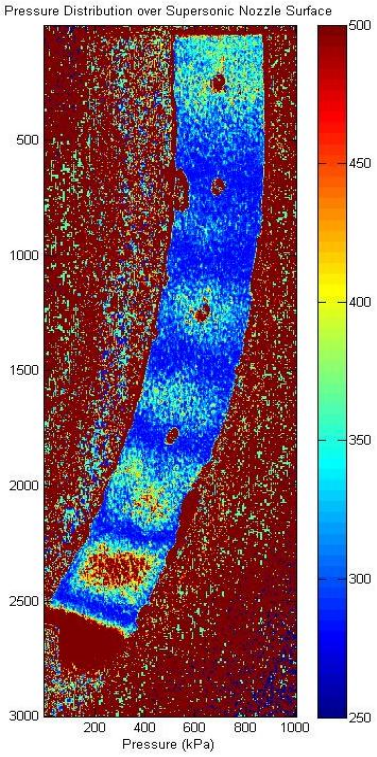

Figure 9. Pressure Ratio image 10 bar case using Fourier solution.

F. Temperature Dependency

Whilst the nozzle surface showed a single state of temperature across the nozzle surface at a given time the temperature was subject to temporal change. The air supply within the canisters cooled over the run-time, changing the temperature of the flow at the inlet. Therefore, in order to determine the temperature dependency of the PSP the effect of the change in temperature over time was examined. Fig. 10. shows a distribution of the pressure ratio measured at the same transverse coordinate over three images captured for the same inlet pressure ratio at varying times.

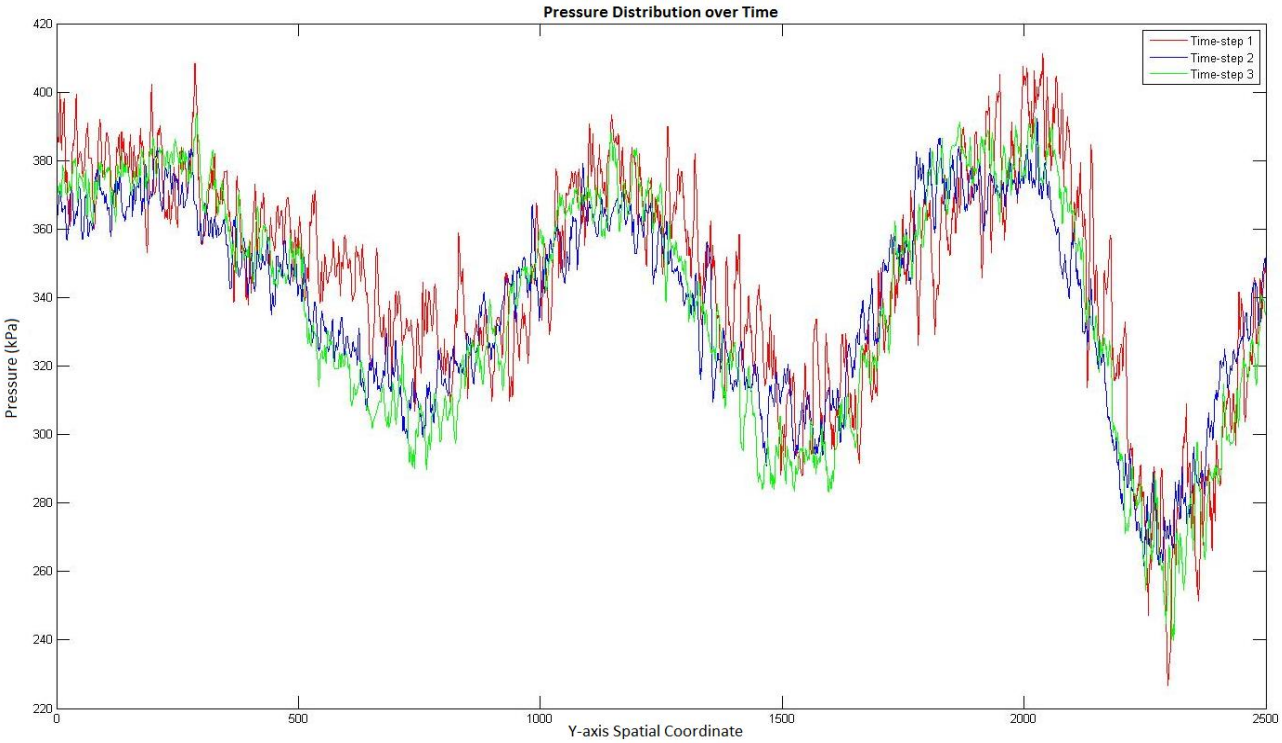

Figure 10. Comparison of pressure distribution of 10 bar case over time.

Table 4. shows the values at nominal points on the surface nozzle for each time case and the deviation measured.

Table 4: Comparison of the pressure distribution and deviation of 10 bar case over time.

Y-axis Spatial Coordinate	Pressure (kPa) – Time Step 1	Pressure (kPa) – Time Step 2	Pressure (kPa) – Time Step 3	Max. Deviation – kPa/%
500	363.022	343.762	352.349	19.26/5.60
1000	349.813	338.630	359.955	21.325/6.30
1500	301.863	313.641	296.099	17.307/5.84
2000	404.640	373.406	377.086	31.234/8.36

For the purposes of this analysis the same Stern-Volmer coefficient values were used for each time-step. This would determine whether any changes occurred due to temperature dependency of the PSP. Ideally if there was no temperature drop there would be no change in pressure. However there is clear change in the measured pressure from each time-step. This is most evident after the first time-step. This is likely due to the rapid cooling of the air canisters from the initial condition. As the flow develops this effect becomes less pronounced. This suggests that the air temperature affects the greatest thermal transfer at the inlet position and through the first shock wave that develops. The maximum deviation measured was 8.36%. However this is likely an outlier result. The trend shown suggests that whilst there is an identifiable temperature effect, the Stern-Volmer coefficients reasonably attributed for this effect. The identified fluctuation could potential be attributed to the air temperature dropping below the limits of the PSP. This can cause a larger variation than expected.

V. Conclusions

In conclusion, the case study analysed shows good agreement with the expected results generated from the CFD solution and experimental flow field results from schlieren images. The expected shock pattern developed within the flow field was shown in the consecutive high and low pressure regions. Whilst the image processing introduced a number of potential sources of error these were largely mitigated through the chosen method intensity ratio system. The smooth filter applied to the image reduced the presence of outlier results and the 2D transverse assumption was within good tolerance outside of the immediate region of the Perspex windows. Whilst the linear solution provided the more agreeable results, the introduction of the Fourier series showed promise, given a more thorough Stern-Volmer coefficient calibration. The temperature dependency of the run-case was also shown to have a measureable effect on the pressure distribution, although to a smaller degree than anticipated. This analysis has shown that PSP is a viable method of analysing the pressure distribution over the nozzle surface. Once the computational program was developed the process of analysis the pressure distribution was shown to be fast and reliable. Analysis shows that for the case the results are both quantitative and qualitatively in agreement with the expected flow field solution.

VI. Recommendations

In future studies it would be worthwhile developing a code in order to determine the best-case solution for the intensity ratio value measured for the nominal pressure tap location. This would reduce the amount of time in re-evaluating this position for each run-case. Whilst it was found that a similar position could be used for this experiment, this process would have to be re-evaluated each time the nozzle reference location was changed, for example in new experimental cases. A potential solution for this is to have a computational solution where the pressure tap location is chosen and the program finds and average intensity from the local intensity values. A method of developing a calibration curve should also be investigated. This will allow the solution to be used for a variety of cases. This curve could then be applied for any 2D flow cases. This could be further developed to provide a three dimensional solution through the use of a calibration matrix across the entire surface face measured.

A study into how to correct the angular image of the nozzle sidewall should be conducted. Whilst the preferable method would be to find a way of mounding the camera so that it retains an unobstructed view of the PSP coated surface given the current experimental conditions this has been unfeasible to date. Therefore a computational method should be developed to provide an image correction so that the painted surface can be viewed from a perpendicular plane. However, as discussed this should be done with minimal interpolation or removal of data captured. Uncertainties introduced due to the method of capturing the images made accurately measuring time dependency difficult. This also introduced problems when trying to correlate the experimental flow images with other methods of flow analysis such as schlieren and CFD images developed. It is recommended that in future cases the camera should be set to run automatically, either through a series of photos taken at given time steps or as a video. This would allow the start time to be measured and images captured at specific run-times for comparative studies. Use of a video requires investigation into the data capacity of the video images and appropriate equipment obtained in order to allow any such images to retain a good signal-noise ratio.

Although limitations are imposed by the nozzle rig used, efforts should be made to regulate the pressure at the nozzle inlet. This could be the physical implementation of a more effective method of controlling the canister pressures or through an analysis done on loses within the rig tubing in order to accurately determine the inlet pressure. It is a recommendation that at the conclusion of this project that further studies be done into quantitatively analysis results garnered from PSP measurements. Work should be done on case studies where conditions are known and the flow field more accurately analysed computationally. This will allow a more thorough comparative study between the PSP measurements and results which have been previously verified.

A final recommendation is that work is done towards analysing the validity and accuracy of a decay-based system. Whilst the intensity-based system provides promising results, the requirement for an accurate temperature correction factor makes its use limited in application. A decay-based system can provide results within a wider scope of applications. The possibility of developing a binary paint that is comprised of both pressure dependent and independent luminophores should also be explored. Whilst not commercially available from the current supplier, a developed paint system will reduce the cost of the paint, reduce issues with the expiry of shelf-life of the product and a tailor made solution to case studies performed.

Acknowledgements

I would briefly like to thank A/Prof Andrew Neely for the guidance given throughout the conduct of this project. I would also like to thank PhD Stud Kyll Schomberg for the contribution of his supersonic nozzle rig, experimental results and time towards the experimental stage. Lastly, I would like to thank PhD Stud Gaetano Currao for assistance in the conduct of the experiment and in post-image processing.

References

[i] Liu, T., Campbell, B. T., Burns, S. P., and Sullivan, J. P., "Temperature- and pressure-sensitive luminescent paints in aerodynamics", Appl Mech Rev vol 50, no 4, April 1997

[ii] Woodmansee, M. A., and Dutton, J. C., "Treating temperature-sensitivity effects of pressure-sensitive paint", Department of Mechanical and Industrial Engineering, University of Illinois, Illinois, July 1997

[iii] Bedwell, B., Davies, A., Dunleavy, M., USPTO, Patent Application for "Pressure sensitive paint", US 20040249593 A1, filed 23 Jan. 2004

[iv] Klein, C. "Application of Pressure Sensitive Paint (PSP) for the determination of the instantaneous pressure field of models in a wind tunnel", Aerosp. Sci. Technol. 4 (2000) 103-109, February 2000

[v] Bedwell, B., Davies, A., Dunleavy, M., USPTO, Patent Application for "Pressure sensitive paint", US 20040249593 A1, filed 23 Jan. 2004

[vi] Schanze, K. S., Carrol, B. F., Korotkevitch, S., "Temperature Dependence of Pressure Sensitive Paints", AIAA Journal Vol. 35, No. 2, February 1997

[vii] Liu, T., Torgerson, S., Sullivan, J., Johnston, R., Fleeter, S., "Rotor blade pressure measurement in a high speed axial compressor using pressure", AIAA Paper 97-0162, January 1997

[viii] Schanze, K. S., Carrol, B. F., Korotkevitch, S., "Temperature Dependence of Pressure Sensitive Paints", AIAA Journal Vol. 35, No. 2, February 1997

[ix] Klein, C., "Application of Pressure Sensitive Paint (PSP) for the determination of the instantaneous pressure field of models in a wind tunnel", Aerosp. Sci. Technol. 4 (2000) 103-109, February 2000

[x] Hradil, J., Davis, C., Mongey, K., McDonagh, C., MacCraith, B. D., "Temperature-corrected pressure-sensitive paint measurements using a single camera and a dual-lifetime approach", Meas. Sci. Technol. 13 (2002) 1552-1557, September 2002

[xi] Klein, C., Engler, R. H., Henne, U., Sachs, W. E., "Application of pressure-sensitive paint for determination of the pressure field and calculation of the forces and moments of models in a wind tunnel", Experiments in fluids (2005) 39: 475-483, May 2005

[xii] Woodmansee, M. A., and Dutton, J. C., "Treating temperature-sensitivity effects of pressure-sensitive paint", Department of Mechanical and Industrial Engineering, University of Illinois, Illinois, July 1997

[xiii] Woodmansee, M. A., and Dutton, J. C., "Treating temperature-sensitivity effects of pressure-sensitive paint", Department of Mechanical and Industrial Engineering, University of Illinois, Illinois, July 1997

[xiv] Schomberg, K,. "Linear expansion-deflection nozzle validation experiments", UNSW, Canberra, February 2014

[xv] Schomberg, K,. "Linear expansion-deflection nozzle validation experiments", UNSW, Canberra, February 2014